Incoherent Resonance Fluorescence from a Rb Atomic Beam Excited by a Short Coherent Optical Pulse

Hyatt M. Gibbs
Bell Laboratories, Murray Hill, New Jersey 07974
(Received 2 January 1973)

Fluorescence has been detected from Rb atoms following narrow-line excitation by a short coherent optical pulse. The fluorescence oscillates as a function of the pulse area A with maxima for $A=\pi$, 3π, 5π, . . . and minima for $A=0$, 2π, 4π, ... In addition to demonstrating one of the simplest coherent optical effects, this experiment dramatizes the potential of the technique for determining dipole moments, pulse areas, relaxation times, and lifetimes. The details of the experimental apparatus are described. Results of a computer simulation of the experiment including the actuai excitation pulse shape, absorption frequency width, finite absorption (5–10% of pulse), and loss to a third level are given.

I. INTRODUCTION

The observation and interpretation of photon echoes[1] underscores the close similarity between the precession of an induced electric dipole moment driven by a coherent optical electric field and the precession of a permanent magnetic dipole moment driven by a coherent radiofrequency magnetic field.[2] In the latter case the sample is generally small compared with the wavelength and the absorption length is long compared with the sample size. Propagation effects are then negligible since all atoms are exposed to the same external field at the same time. In the optical regime the typical sample dimension is large compared to the wavelength, and the absorption length is often shorter than the sample dimension. Propagation effects then play a central role, as illustrated clearly by self-induced transparency (SIT).[3,4] In SIT, an input coherent optical pulse of area 2π with a hyperbolic secant time dependence induces its way slowly (compared with its vacuum velocity) through the sample without loss. This is sometimes pictured as excitation by the first half of the pulse followed by coherent deexcitation by the second half so that no energy remains in the absorbers. Mathematically, this coherent optical phenomena requires a simultaneous or self-consistent solution of the equations of Maxwell (in which the source term accounts for the effect of the absorbers on the field) and Schrödinger (in which the field changes the states of the absorbers). SIT has been studied in detail via experimental demonstrations and computer simulations.[4]

The experiment described herein is simpler than SIT in that the sample is optically thin and so can be described by Schrödinger's equation alone. Propagation effects are unimportant; all atoms undergo the same evolution. The coherent optical field excites each atom to an initial state (rotates the pseudopolarization through an initial angle θ_0). During or after the pulse, the atom can spontaneously radiate its excitation. This fluorescence can be used to monitor the polarization of the atoms. In particular, the total fluorescence following the pulse is a measure of the final polarization or final tipping angle. It is essential that the optical pulse be coherent and shorter than the radiative lifetime if the fluorescence is to be an oscillatory function of the input area. The present experiment closely approximates the ideal case in which the fluorescence is a maximum for input areas of π, 3π, etc., and zero for 0, 2π, 4π, ... This simple coherent optical phenomenon demonstrated here should be a useful technique for determining dipole moments, pulse areas, relaxation times, and lifetimes, depending upon which is unknown.[5]

The details of the experimental apparatus and technique are presented in Sec. II, the quantum-electrocynamical (QED) theoretical predictions in Sec. III, and a comparison of data and predictions in Sec. IV.

II. EXPERIMENTAL DETAILS

Many of the details of the apparatus have already been published.[4,6] The primary alterations were frequency stabilization (±2 MHz) of the Hg laser by locking it to the center of a Rb atomic-beam absorption line and detection of the fluorescence by single-photon counting techniques.

The interaction of the laser beam and Rb atomic beam is pictured in Fig. 1 along with details of the atomic-beam oven. The atomic beam at the intersection was about 0.27 mm high and had a density of $\approx 10^{10}$ atoms/cm^3. The spatial dimensions of the beam oven were dictated by the fact that the oven operated within the 3.6-cm-diam bore of a superconducting magnet. A field of about 75 kOe is required to Zeeman tune the Rb D_1 absorption line

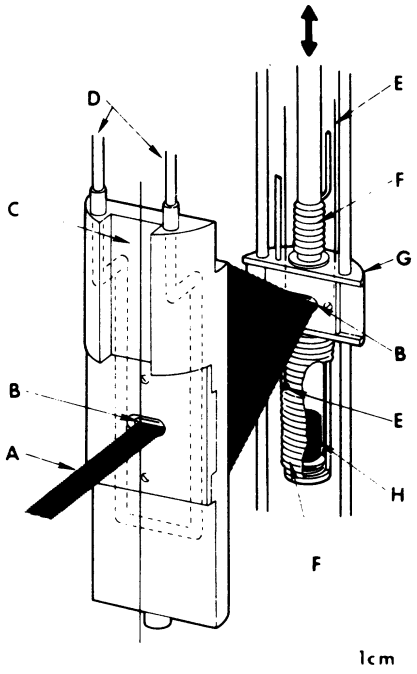

FIG. 1. Sketch of atomic-beam apparatus and intersection of light and atom beams. The 1-cm separation between oven and beam slits is exaggerated for clarity. A, Rb beam; B, slit; C, laser beam; D, coolant lines; E, thermocouple; F, heater; G, atomic-beam oven; H, Rb in Pyrex tube.

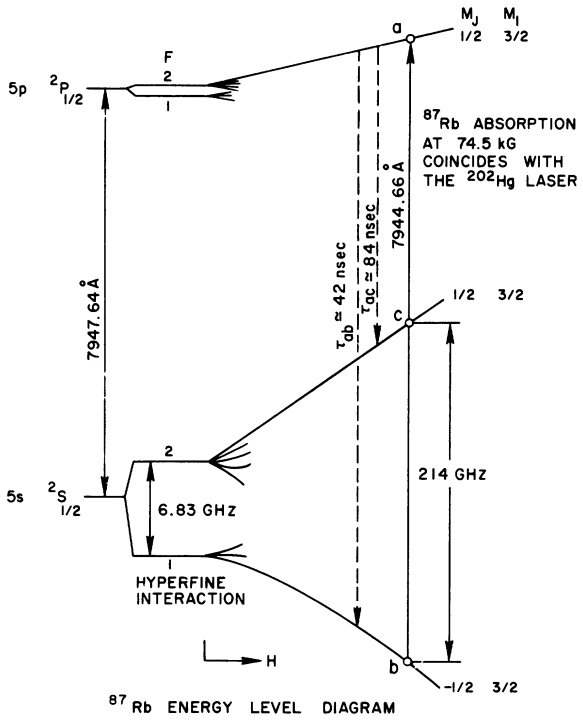

FIG. 2. Diagram of the relevant energy levels of ^{87}Rb as a function of magnetic field strength. The Zeeman interaction at 74.5 kOe lifts the low-field degeneracy and increases the absorption frequency to coincide with the laser emission frequency.

into coincidence with the Hg laser (Fig. 2). A typical magnetic scan of the Rb absorption showing the four ^{87}Rb and six ^{85}Rb resolved components constitutes Fig. 3. Most of the data were taken using the well-resolved lowest-field ^{87}Rb absorption line. Only ^{87}Rb atoms with $M_I = 3/2$ participated in the experiment; the remaining atoms were useless but harmless.

The observed width of 15 MHz was several times narrower than the frequency spread of the pulse (but 2.5 times broader than the homogeneous width of 6 MHz from the natural lifetime); computer simulations indicated little improvement would result by reducing the width to 1.5 MHz. That is, the sharp-line condition needed for all atoms to see the same optical pulse was well satisfied experimentally.

A summary block diagram of the apparatus is shown in Fig. 4. The efficacy of the laser locking system is discussed in Sec. II A. The ±2-MHz stability was more than sufficient for the current observations of excitation of a 15-MHz-wide absorber by a short optical pulse with frequency spread close to 100 MHz. In Sec. II B are described the steps taken to achieve spatial uniformity of the optical pulse so that fluorescence is observed only from atoms exposed to pulses of the same area. The temporal profile of the optical pulse is presented in Sec. II C and the single-photon-counting equipment in Sec. II D. Many other aspects of the experiment, such as tests for phase shifts in the incident pulse, Fabry–Perot observations of the optical pulse, etc., are discussed in Ref. 4.

A. Laser-Absorber Locking

The locking of the laser to the beam absorption was accomplished as follows. Mirror M_1, was modulated piezoelectrically at 22.5 Hz, shifting the laser frequency by several MHz above and below the central frequency (weak modulation of the single-mode selector at C1 would affect the amplitude, not the frequency). If the mode frequencies of the long (M_1 to M_2) and short (single-mode selector at C1 to M_2) cavities were not coincident,

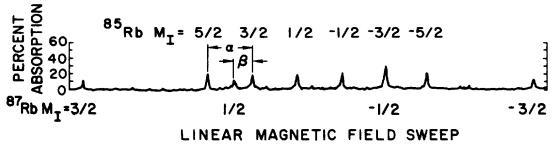

FIG. 3. Absorption of right circularly polarized low-intensity laser light through an atomic beam of natural Rb as a function of magnetic field.

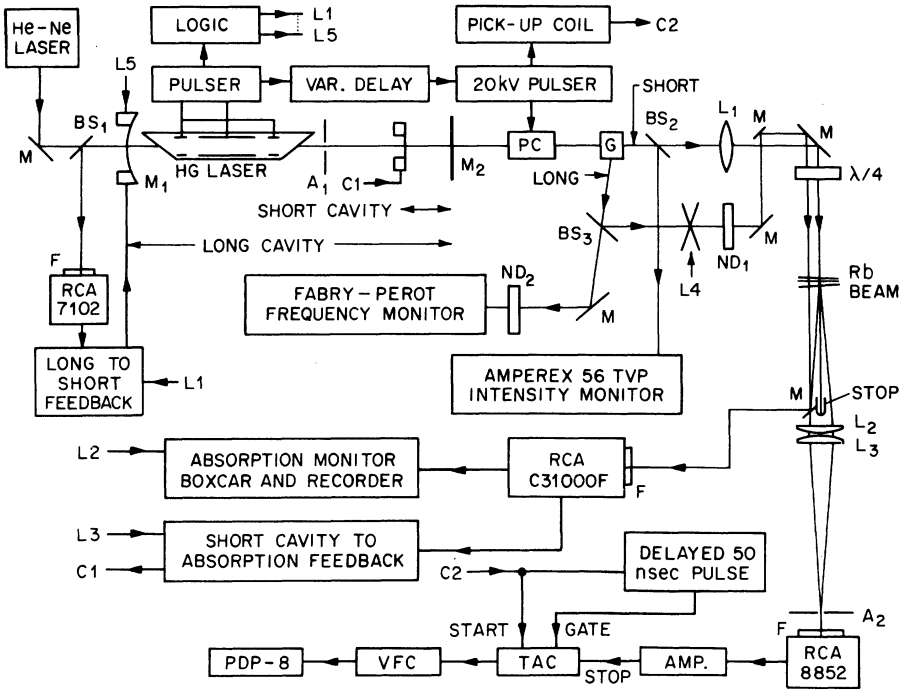

FIG. 4. Block diagram of experimental apparatus. A_1, aperture to select TEM_{00}; A_2, aperture to select fluorescence from central, uniform portion of excitation region; BS_i, ith beam splitter; Ci, ith control signal; F, 7945-Å, 100-Å interference filter; G, Glans prism; Li, ith logic pulse; L_i, ith lens; M, mirror; M_1, 3-m totally reflecting mirror; M_2, 4% transmission flat output mirror; ND_i, ith neutral density filter; PC, Pockels cell; TAC, time-to-amplitude converter; VFC, voltage-to-frequency converter.

an error signal was detected by the 7102 photomultiplier and the long-cavity length adjusted to the center of the short-cavity bandpass. A time constant of about 3 sec was used for the lock-in amplifier in this feedback loop. The same modulation of the laser frequency was also used to detect (with the C31000F) an error signal whenever the laser frequency was not centered on the absorption of a weak-intensity 1-μsec-long Hg laser pulse by the Rb atomic beam. But a time constant of 30 sec was used in this short-cavity to beam-absorption feedback loop. This prevented changing the short-cavity length by mistaking a long-cavity drift for a short-cavity drift. Feedback corrections were maintained at a fraction of a mode by manual voltage corrections every few minutes. A logic control system and chopper separated in time the locking from the fluorescence observations. That is, no voltage was applied to the piezoelectric crystals supporting M_1 and the 1-μsec laser pulse was not permitted into the magnetic bore during the observation of the fluorescence from the short excitation pulse (see Fig. 5).

The fact that the laser is on for only 1 μsec every 10 msec complicated and limited the capability of the locking system. But the long-term stability was quite adequate for this experiment, as shown in Fig. 6.

The use of two beams permitted the use of a 500-μ slit and 30-MHz absorption width for the

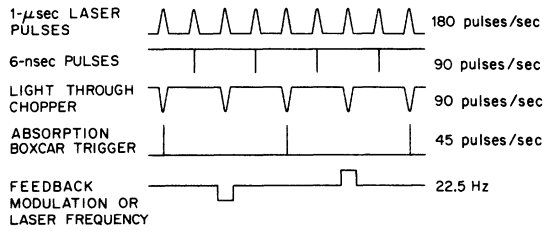

FIG. 5. Synchronization of laser and control pulses. The long pulse used for locking the laser to the absorption-line center was not on during the 6-nsec excitation pulse or subsequent fluorescence monitoring. The absorption of the long pulse was monitored and the experiment performed with no voltage applied to the end-mirror piezoelectric crystal. The feedback signal for locking the laser to the absorber was obtained by shifting the laser frequency up and then down by the same amounts in between fluorescence and absorption measurements.

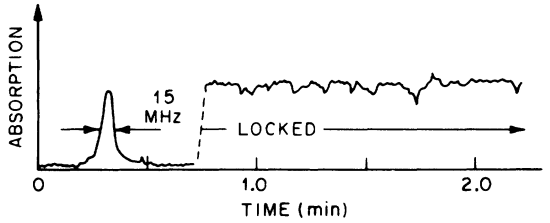

FIG. 6. Laser-absorber frequency locking. The first portion of the scan illustrates the 15-MHz absorption width when the field is scanned with the laser free running. When the laser frequency is locked to the center of the atomic-beam absorption, the absorption remains close to its maximum value. The frequency difference between the laser and absorber is certainly much less than ±7.5 MHz for which the absorption would be one-half its maximum value.

long-pulse feedback beam rather than the 200-μ slit and 15-MHz width needed for the short pulse to satisfy the sharp-line condition. This gave larger absorption for the long pulse, improving the feedback signal-to-noise ratio. On the other hand, the two optical beams intersect the atomic beam at different positions in the magnetic field. That the difference in field might result in a significant shift was not appreciated at first and considerable data were taken 20 MHz off resonance. In the later runs the feedback optical beam was moved to a position with the same field as that of the short-pulse beam. This was verified before and after each run by simultaneously recording the absorptions of the long and short pulses. (Of course, the long and short pulses have orthogonal linear polarizations as they emerge from the Glans prism. Two linear polarizers were used to convert some of the long pulse into the same polarization as the short pulse, so both pulses were right circularly polarized after passage through the quarter-wave plate. Also, to prevent optical pumping by the long pulse, its intensity was kept low by using a glass slide for beam splitter BS_3 and inserting neutral density filters ND_1).

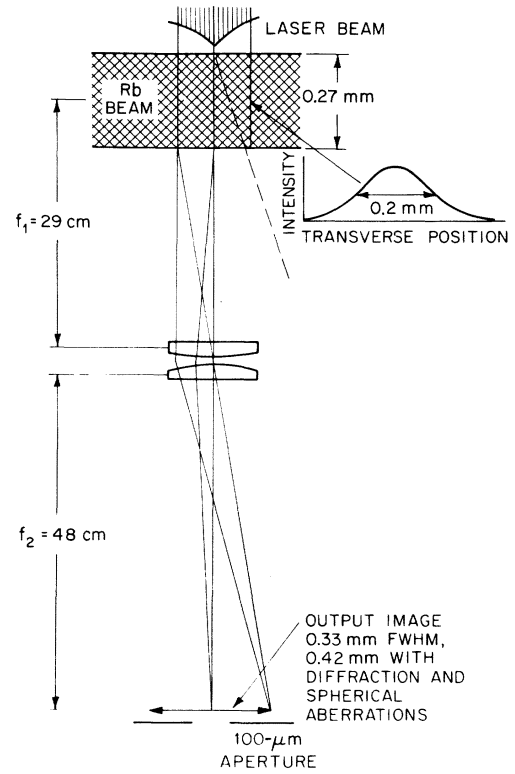

FIG. 7. Uniform plane-wave approximation. The fluorescence emanating from the excited beam atoms was imaged on a 100-μm aperture. The acceptance half-angle was always less than 3°, so that the aperture passed fluorescence only from atoms excited by the central, uniform portion of the laser beam. If a large acceptance angle were permitted, such as the dashed line, it would be impossible to distinguish fluorescence originating in the central portion from fluorescence coming from less strongly excited atoms. The small acceptance angle also restricted the fluorescence almost entirely to the 7944.6-Å ($\Delta M = -1$) transition since the 7950.7-Å ($\Delta M = 0$) radiation is much smaller within that angle. Plano-convex lenses were used with the object and image at the focal lengths to minimize spherical abberrations.

B. Spatial Uniformity of Optical Excitation Pulse

One of the problems in the experiment is to satisfy the uniform plane-wave condition. That is, in order that all atoms be excited to the same superposition of ground and excited states, one must make sure that every atom is exposed to the same optical field for the same time. But the frequency-stabilized laser was operated in the lowest-order TEM_{00} transverse mode which has a Gaussian spatial profile. The uniform plane-wave condition was then approximated by observing only fluorescence from atoms excited by the uniform central portion of the profile. This was done by imaging the fluorescence upon an output aperture as shown in Fig. 7. The profile of the fluorescence at the output aperture was about the size expected from diffraction and spherical aberrations and the magnification of the lens system. The spatial profile in Fig. 8 is compared with the 100-μm diameter of the output aperture.

It would appear simpler to place an aperture just above the atomic beam to prevent the nonuniform portions of the laser beam from exciting the Rb. This was tried, but two problems made that method less practical. First, the aperture, which had to be less than 100 μm in diameter because of the power limitations of the laser, did not really result in a uniform excitation because of Fresnel diffraction. This was reduced to

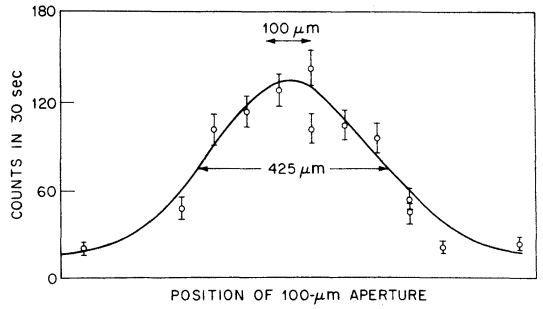

FIG. 8. Experimental transverse spatial profile of the forward fluorescence imaged as in Fig. 7. Vertical and horizontal profiles were obtained at the start of each run to position the 100-μm aperture on the peak of the profile.

roughly acceptable levels by placing the aperture adjacent to the atomic beam. But this aggravated the second problem. The fluorescence in Rb is at the same frequency as the excitation pulse. An aperture placed at the atomic beam inevitably scatters some of the excitation pulse into the fluorescence detectors. The fluorescence is necessarily a small fraction of the excitation pulse since it is emitted in all directions and because the absorption of the incident pulse must be small. Low absorption is necessary in order that all atoms through the sample be subjected to the same integrated electric field and so radiation trapping is negligible. Even with a parabolic reflector to increase the collection solid angle for the fluorescence, the scattered excitation pulse was much larger than the fluorescence. Experimentally it was found much easier to discriminate against the excitation pulse by the scheme of Fig. 7.

The output imaging lenses in Fig. 7 were placed in the beam in such a way as to minimize spherical aberrations. They were held concentrically in one holder with their flat surfaces parallel to each other and perpendicular to the laser beam (observed by the back reflection of the visible alignment laser). They were positioned such that the image with them was on the same axis as the laser beam in their absence. Profiles were taken for various z positions (along the beam) of the 100-μm aperture to verify the location of the image plane. With an aperture in the position of the atomic beam, the output image reproduced the Fresnel diffraction discussed above. In addition, a few curves of integrated fluorescence versus input area were taken for various placements of the aperture along the z axis to verify that the best position was used. Finally, transverse profiles were taken before each run to center the aperture on the focussed fluorescence.

C. Temporal Profile of Excitation Pulse

Just as important as the spatial profile of the excitation optical pulse is its temporal profile. In the ideal case the optical pulse duration would be negligible compared with the radiative emission time (about 28 nsec here). In the present experiment this is not the case (see Fig. 9). The full width at half-maximum (FWHM) of the intensity of the pulse is only 7 nsec, but there is a weak tail. Also, the electric field is proportional to the square root of the intensity, so that its FWHM is closer to 10 nsec. It would be desirable to eliminate the tail in an improved experiment. Here it has been included in the computer simulation. The tail was reduced considerably from earlier self-induced transparency experiments by improving the electrical matching of the Pockels-cell driver.

Improved experiments might also shorten the main pulse. The low power of the laser and diffraction complications with tighter focusing of the laser beam made such a reduction difficult in the present experiment.

Real-time observations of the pulse with a fast silicon photodiode revealed that the shape of the pulse was highly reproducible and its amplitude exhibited the same 5–10% jitter as the long pulse from the laser.[4] The amplitude of the short pulse was decreased by triggering the Pockels cell at a later time on the long pulse.[4]

The area of the excitation pulse was then highly reproducible from pulse to pulse, so that even with slight averaging by the finite acceptance angle, diffraction, and finite output aperture the uncertainty in area was no more than ±10%. Since the theoretical integrated fluorescence does not vary rapidly as a function of input area in this experiment, no convolution was necessary in comparing the theoretical fluorescence-versus-area curve with observations.

D. Single-Photon Counting

The fluorescence detection system used standard single-photon counting instrumentation. The

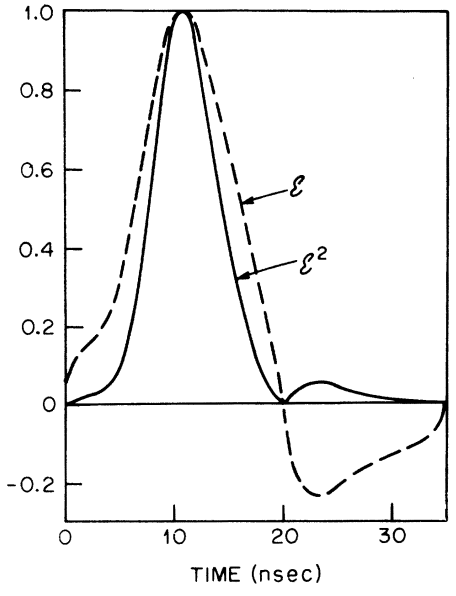

FIG. 9. Input intensity ($\propto \mathcal{E}^2$) and electric field ($\mathcal{E}$) used in the computer simulation. The intensity profile was determined by experimental single-photon counting of the input pulse. The change of sign of $\mathcal{E}$, which is reasonable from the shape of the intensity and the expected continuity of $\mathcal{E}$, was verified by detecting the sign reversal of the voltage applied longitudinally to the Pockels cell. For a dipole moment $p = 4.35 \times 10^{-18}$ esu cm, the intensity units are W/cm^2 for a pulse of area 1.35π.

pulse induced in a pickup coil by the firing of the Pockels-cell thyratron started a time-to-amplitude converter (TAC). The arrival of a pulse from the fluorescence 8852 photomultiplier (-2400 V) stopped the TAC. A voltage-to-frequency converter and computer-controlled up counter converted the TAC output into a time channel (50, 2 nsec apart). One count was then added to that channel. The computer stored and displayed this fluorescence decay.

The counting rate was always at least 10 (usually 50–100) times slower than the 90 counts per second rate of the excitation pulse, preventing pile-up distortions. Some of the difficulty in reducing counts from reflections of the input pulse into the detector were described in II B. A blackened tube stop (see Fig. 4) reduced the input-pulse light reaching the detector by 5000. Insertion of the 100-μm aperture reduced it further. Finally time discrimination was used for many of the runs to ignore all counts during the first 22 nsec. Data taken without the time discrimination revealed that for an input area of π the leakage light was smaller than the fluorescence. But at 3π the leakage is about 10 times more intense and large compared with the fluorescence during the first 20 nsec.

Thus, with care the reflected light was reduced to an unimportant level. No doubt a system in which fluorescence could be observed on another, different wavelength, transition would be much simpler. There is in this experiment fluorescence at 7950.6 Å from the $^2P_{1/2}$ ($M_J = +\frac{1}{2}$) to $^2S_{1/2}$ ($M_J = +\frac{1}{2}$) transition. But its angular distribution is zero in the forward direction and maximum at right angles. With an aperture close to the atomic beam and the parabolic reflector (see II B), the output fluorescence was observed through a 3-Å-wide 7950-Å interference filter. But the discrimination against the 7945.6-Å excitation pulse was inadequate, probably because the filter works effectively only for parallel light. Neither the reflected leakage light nor the fluorescence after reflection from the imperfect reflector was parallel. In the scheme used, fluorescence was accepted only in a small forward cone in which the 7950.6-Å fluorescence was negligible.

The single-photon-counting apparatus was time calibrated by measuring the delay of a repetitive stop pulse on a Tektronix 564 sampling oscilloscope. The latter was calibrated with a Tektronix 184 time-mark generator.

III. COMPUTER SIMULATION

In Refs. 5 and 6 it is shown that coherent excitation of two-level sharp-line absorbers through a tipping angle or input area

$$\theta(0) \equiv (2p/\hbar)\int_{-\tau}^{0} \mathcal{E}(t)\,dt \tag{1}$$

in a time τ short compared with relaxation times yields an initial population in excited state a of

$$\rho_{aa}(0) = [\sin \tfrac{1}{2}\theta(0)^2]\,. \tag{2}$$

$\mathcal{E}(t)$ is the slowly varying amplitude of the electric field and p is the electric dipole moment of the transition between ground state b and excited state a.[3,4] In the Weisskopf–Wigner QED approximation, the excited state spontaneously decays as

$$\rho_{aa}(t) = \rho_{aa}(0)\,e^{-t/\tau_{ab}}, \tag{3}$$

with characteristic time[4]

$$\frac{1}{\tau_{ab}} = \frac{8}{3}\left(\frac{\omega^3}{\hbar c^3}\right)p^2, \tag{4}$$

where ω is the angular frequency of the transition. The QED fluorescence rate is given by

$$F_{\mathrm{QED}}(t) = (N_2\hbar\omega/\tau_{ab})\,\rho_{aa}(t), \tag{5}$$

where N_2 is the number of two-level atoms. Thus QED predicts a single exponential decay independent of the area of the input pulse which determines the probability that the atom is in the excited state. The integrated fluorescence out to time T

$$\int_{t'}^{t'+T} F_{\mathrm{QED}}(t)\,dt \propto (\sin \tfrac{1}{2}\theta)^2 \tag{6}$$

is the same oscillatory function of θ independent of the initiation time (t') or duration (T) of the integration (see Fig. 10). The integrated fluorescence is then expected to be zero for $\theta = 0,\ 2\pi,\ 4\pi, \ldots$ and a maximum for $\theta = \pi,\ 3\pi, \ldots$. The experimental deviations from the ideal two-level sharp-line absorber excited by a very short optical pulse were taken into account in the computer simulation as discussed next. But the actual experiment was reasonably close to the ideal system and did in fact verify the single exponential decay

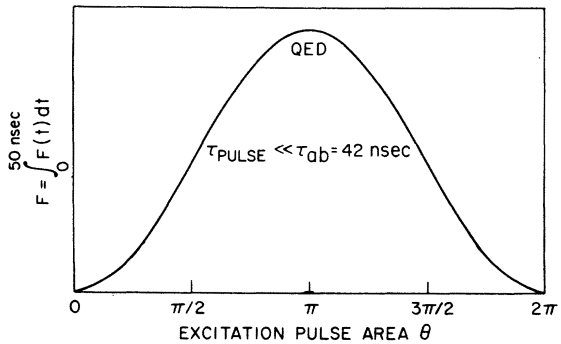

FIG. 10. Integrated fluorescence of a sharp-line two-level transition following rapid excitation by a pulse of area θ (theoretical).

and the oscillatory dependence of the integrated fluorescence upon input pulse area.

The ^{87}Rb atoms in high field are to a good approximation three-level absorbers.[4] The frequency spread of the pulse was five to ten times broader than the 15-MHz beam absorption width, so the sharp-line condition was closely approximated. The sample was optically thin. But the excitation pulse ($\lesssim$ 7-nsec FWHM) had nonzero intensity for about 35 nsec, comparable to the 28-nsec excited-state lifetime. The two primary deviations from the ideal simple experiment were the excitation pulse length and the absorber's third level c. But all four of these departures from the ideal system were included in the computer simulation, permitting their relative importances to be investigated easily.

The coupled Schrödinger and Maxwell equations lead to the following equations[4]:

$$\dot{u} = v\,\Delta\omega - u/T_2' \ , \tag{7a}$$

$$\dot{v} = -u\,\Delta\omega - \kappa^2\,\mathcal{E}W/\omega - v/T_2' \ , \tag{7b}$$

$$\dot{W} = v\mathcal{E}\omega - (x+W)/T_1 \ , \tag{7c}$$

$$\dot{x} = -(2/T_2' - 1/T_1)(x+W), \tag{7d}$$

$$\frac{\partial \mathcal{E}}{\partial z} + \frac{1}{c}\frac{\partial \mathcal{E}}{\partial t} = -\frac{2\pi\omega}{c}\int_{-\infty}^{\infty} g(\Delta\omega)v(\Delta\omega)d(\Delta\omega). \tag{8}$$

Thus the external field is treated classically. Quantization of the electromagnetic field enters only in the incoherent spontaneous emission. The pseudopolarization vector $\vec{P} = u\hat{u}_0 + v\hat{v}_0 - (W\kappa/\omega)\hat{w}_0$ has components

$$u + iv = \tfrac{1}{2}Np\,\langle \sigma_x + i\sigma_y \rangle = Np\ \rho_{ba} = Np\ \rho_{ab}^* \tag{9a}$$

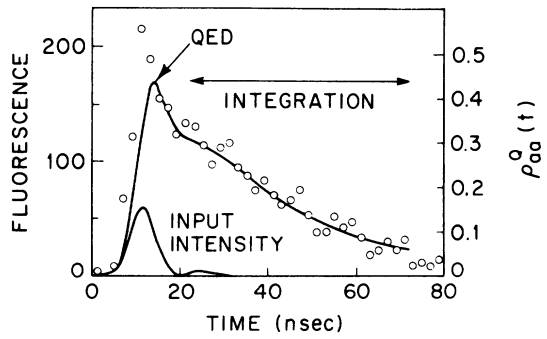

FIG. 11. Comparison of $F_{\rm QED} \propto \rho_{aa}(t)$ with experimental data for an input pulse area of π. The input pulse is shown in more detail in Fig. 9. Reflections of the excitation pulse into the detector added counts to the fluorescence signal in the 5–15-nsec region. The theoretical curve is a computer simulation for the actual three-level system including 15-MHz absorption width, finite absorption, and the actual input pulse. The theoretical curve is normalized to equal the data at 35 nsec, after which the external field vanishes.

and

$$W = = \tfrac{1}{2}N\hbar\omega_0\,\langle \sigma_z \rangle = \tfrac{1}{2}N\hbar\omega_0(\rho_{aa} - \rho_{bb}). \tag{9b}$$

Also,

$$x = \tfrac{1}{2}N\hbar\omega_0\,\langle I \rangle = \tfrac{1}{2}N\hbar\omega_0(\rho_{aa} + \rho_{bb}), \tag{9c}$$

$$\frac{1}{T_1} = \frac{1}{2\tau_{ac}} + \frac{1}{\tau_{ab}}, \tag{10a}$$

$$\frac{1}{T_2'} = \frac{1}{2\tau_{ac}} + \frac{1}{2\tau_{ab}}, \tag{10b}$$

$$\kappa = 2p/\hbar. \tag{10c}$$

N is the number of three-level atoms; $\rho_{bb}(0) = \rho_{cc}(0) = \frac{1}{2}$. $\mathcal{E}$ is the slowly varying envelope of the electric field of carrier frequency ω incident upon absorbers with frequencies $g(\omega)$ centered about ω_0. The radiative emission terms in Eqs. (7) were obtained in Ref. 4 in the Weisskopf–Wigner approximation following Mollow and Miller. Equation (8) describes the effect of the absorbers on the field in an optically thick sample; the effects of having a finite (but thin) sample were included and studied via Eq. (8).

The results of the computer simulations will be presented with the data in Sec. IV.

IV. COMPARISON OF EXPERIMENTAL DATA AND COMPUTER SIMULATIONS

A. Observations

1. Time Dependence of Fluorescence Decay

The number of fluorescence counts following within each 2-nsec decay channel are shown in Fig. 11 for an excitation area of about π. The results are in excellent agreement with theory except in the 6–14-nsec interval, where light scattered from the incident pulse adds counts that are not fluorescence. That this was the case was verified by its presence with the atomic beam blocked. Also it increased linearly with the incident pulse intensity unlike the resonance fluorescence (see Fig. 12).

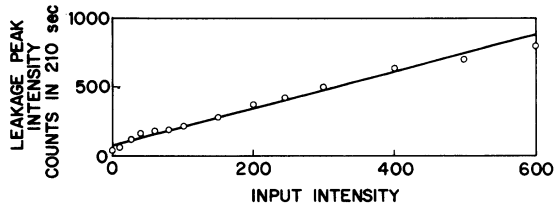

FIG. 12. Demonstration that the leakage intensity between 5 and 15 nsec in Fig. 11 increases linearly with input intensity unlike the integrated fluorescence (Fig. 14).

Several decay curves (beyond 35 nsec) for various input areas have been least-squares fitted to a single exponential. The best-fit lifetimes are consistent with the prediction of QED that the decay should be an exponential with 28-nsec decay time independent of the input area.[6]

It is interesting to compare theoretical simulations under various conditions to see how closely complete inversion of the a-b system is approached. Figure 13 illustrates the time evolution of ρ_{aa} and ρ_{bb} ($\rho_{aa}+\rho_{bb}+\rho_{cc}=1$). The inversion at the end of the tail of the pulse is not large because of spontaneous emission during the pulse. An even lower inversion results 20 MHz off resonance.

2. *Integrated Fluorescence*

The fluorescence was electronically integrated from 22 to 72 nsec and recorded as a function of input-pulse intensity or area as in Fig. 14. Many more integrated-fluorescence data were taken than decay curves. The averaging effects of only approximating the uniform plane-wave condition and of amplitude fluctuations of the laser are conservatively indicated by the horizontal error bars in Fig. 14. This averaging is more detrimental where the input area is larger since the absolute uncertainty in angle becomes a larger fraction of π. The data above 3π are also slightly less certain because in order to obtain sufficient power, it was necessary to increase the Pockels-cell voltage and to remove a linear polarizer used to improve the purity of the laser output polarization. Also at higher pulse intensities the details of the pulse shape become more important. The computer simulation is seen to be in good agreement with the experimental data.

The minimum at 2π is not zero because of spontaneous emission during the excitation pulse. The maximum at 3π is higher than at π, because under the action of the 3π pulse the atom has less probability of being in the excited state from which spontaneous decay occurs. For higher areas than shown, the integrated fluorescence should approach a constant saturated value corresponding to half-excited atoms with no macroscopic polarization. It appears that the saturated value is slightly lower than the peak at π, again indicating that at π there is a macroscopic polarization just slightly above the equator. This should also emphasize that the area π refers to the *input* area; its effect on the atoms is not to invert them completely because of the incoherent spontaneous emission during the excitation. But the essential features of the expected oscillations of the fluorescence-monitored polarization as a function of the initial precession angle determined by the input-pulse area are clearly seen and demonstrate the similarity between optical precession and magnetic precession.

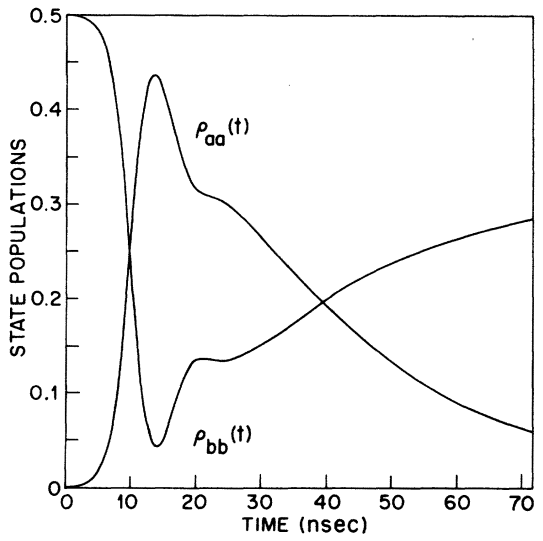

FIG. 13. State-population time dependence for an input-pulse area of π. Since ρ_{cc} is 0.5 or greater, ρ_{aa} must be no larger than 0.5. Because of the negative tail, the polarization is rotated by about 1.25π and then by -0.25π. The first time the pulse area passes through π, $\rho_{aa}\approx 0.435$ and $\rho_{bb}\approx 0.044$ at $t\approx 13.5$ nsec, and the a-b system is almost completely inverted. At the end of the pulse ($t=35$ nsec) when the area is again π, ρ_{aa} is only 0.225 because of spontaneous emission from a to b and c during the pulse. Nonetheless, the a-b system is left slightly inverted. A ρ_{aa} as high as 0.37 (out of 0.5) is predicted by the computer simulation at the end of the positive portion of $\mathcal{E}(t)$.

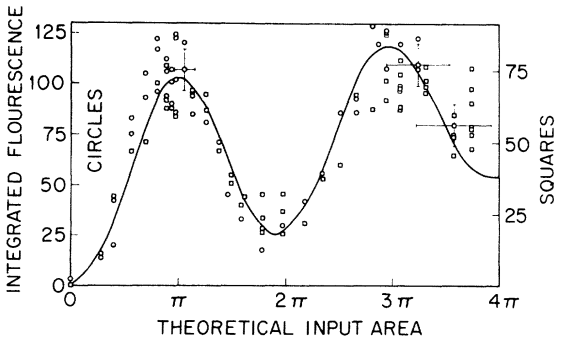

FIG. 14. Fluorescence integrated from 22 to 72 nsec (see Fig. 9) as a function of input-pulse area. The squares and circles are counts in 100- and 80-sec intervals for peak continuous-wave absorption coefficients of 0.21 and 0.32, respectively. The simulated curve is normalized to yield a minimum weighted variance with the circled points of 2.2. The areas assigned to the experimental points in order to agree with the shape of the theoretical curve are in good agreement with the areas deduced from observations of self-induced transparency (see Fig. 16).

Also, data taken 20 MHz off resonance are in reasonable agreement with the simulation (see Fig. 15). Since the input pulse is not hyperbolic secant in its time dependence, it is unable to return the polarization as close to its initial value when it is off resonance as when it is on resonance, i.e., the minimum in Fig. 14 is deeper than in Fig. 15. For the same reason there is an off-resonance contribution to the effective field resulting in one complete rotation of the polarization vector before the area of the input pulse is 2π, i.e., the minimum in Fig. 15 occurs at about 1.6π compared with $\approx 2\pi$ in Fig. 14.

In the discussion so far, no calibration of the input area has been introduced. Rather the first minimum in the experimental fluorescence was identified as the first minimum in the computer simulation. Self-induced-transparency observations reported in Fig. 16 verified that the input area for the first peak in Fig. 14 was indeed π.

B. Error Estimates

1. *Statistics of Small Number of Atoms*

One might worry about density fluctuations within the small volume ($\approx 10^{-6}$ cm^3) of the beam irradiated. But with a typical density n of 10^{10} atoms/cm^3 there were $\approx 10^4$ atoms, so that the fluctuations should have been of order 1%.

2. *Spin Exchange and Resonant Collisions*

The time between spin-exchange collisions should be of order $(\sigma n v)^{-1}$, where the exchange cross section is of order 2×10^{-14} cm^2. This yields 0.1 sec.[7] Resonant broadening collisions between excited and ground-state alkali-metal atoms can have cross sections of order 10^{-12} cm^2.[8] But for the beam densities used, the time between collisions would be 1 msec. Thus collisions between Rb atoms were too infrequent to affect the results in any way. Collisions with background gas atoms of comparable density would be even less important because the cross sections are smaller.

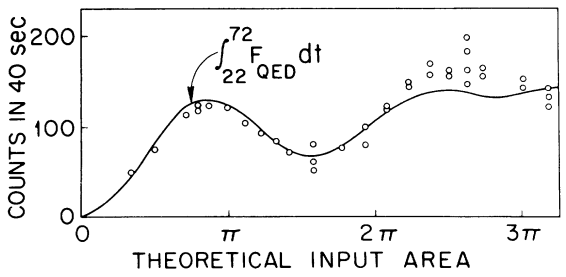

FIG. 15. Integrated fluorescence with the laser frequency 20 MHz below the center of the absorber frequency. The experimental points (circles) are in reasonable agreement with the predictions (solid curve).

3. *Atomic Motion*

Observation of fluorescence occurred out to 72 nsec after the pulse was turned on. During that time a Rb atom with the mean velocity in the beam would travel 30 μm. Since this distance was small relative to the 200-μm full-diameter-at-half-maximum intensity of the excitation beam, the averaging of the electric field by the displacement of an atom during the observation period was negligible.

4. *Coherent Resonance Fluorescence*

Atoms in the same state and sufficiently close in space can cooperatively emit their excitation via coherent resonance fluorescence in a time much shorter than the spontaneous lifetime.[9] But for an optically excited two-level system, as the density becomes high enough to observe coherent resonance fluorescence, self-induced transparency occurs.[10] That is, the excitation pulse makes its way through the sample by coherent absorption and reemission, so it is impossible to excite all of the sample to the same initial state from which coherent resonance fluorescence can occur for the en-

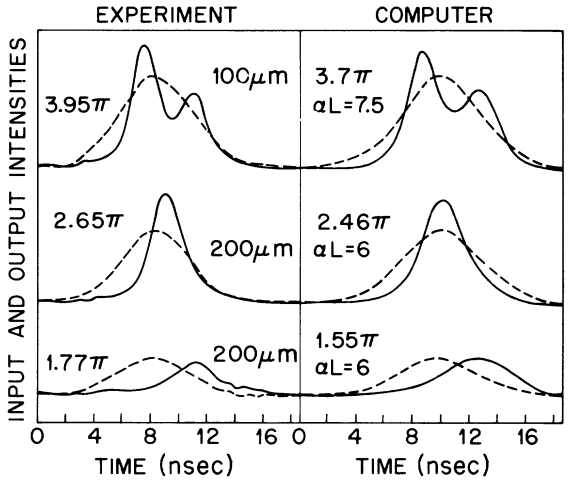

FIG. 16. Self-induced transparency in an optically thick beam verifying that the integrated-fluorescence minimum occurs at an area of 2π. The larger slit used to increase the absorption resulted in a 45-MHz absorption width. The absorption coefficients αL used in the computer simulation were experimental values that could be slightly low if unabsorbable left circularly polarized light were present in the incident beam. The best agreement between the observations and the simulation is obtained for an input area slightly smaller than the experimental identification from Fig. 14 and a 20 or 30% higher αL. But these differences are well within the uncertainties.

tire sample. Coherent resonance fluorescence is included in the simultaneous solution of Maxwell's and Schrödinger's equations used in the computer simulation. But its effect was small since the simultaneous solution differed little from the solution of Schrödinger's equation alone.

Experimentally the integrated fluorescence was found to be independent of the density (Fig. 14), and the exponential lifetime was 28 nsec for all input areas. Furthermore, the power ratio of the coherent to incoherent resonance fluorescence is estimated to be at most 10–20% even at its maximum value for an input area of $\frac{1}{2}\pi$.[9] Finally the coherent fluorescence is emitted in a narrow cone in the forward direction. The incoherent fluorescence observed outside that cone accounted for all of the absorbed energy. The power for a π pulse was about 0.75 W/cm^2, the pulse absorption was 6%, and the solid angle permitted into the detector was 0.35×10^{-3}. Then with each excitation of the beam, about eight of the photons emitted from the excited region were imaged on the 100-μm output aperture. The $\approx$3% quantum efficiency, loss of a factor of 4 or 5 in windows, lenses, filters, and mirrors, and 90 pps repetition rate of the laser yield about 5 counts per second predicted if none of the absorbed energy is emitted coherently. The observed counting rate agreed with this estimate to well within the factor of 2 or 3 guessed accuracy of the estimate.

V. CONCLUSIONS

Oscillations as a function of input-pulse area have been observed in the fluorescence from Rb atoms after coherent narrow-line excitation by a short optical pulse. This demonstration of a simple coherent optical effect could have several uses. Knowledge of the time dependence of the electric field envelope would permit one to determine the dipole moment from the area found by this technique. Conversely, if the dipole moment is known, the time integral of the envelope could be found even when it varies too rapidly to be observed directly. If the relaxation times are too short to be observed directly, information could still be gained by observing the elimination of the 2π minimum with reduced relaxation times. The minimum disappears when most of the atoms are removed from the precessing polarization by relaxation before they have been rotated through an angle of 2π, i.e., coherently excited and deexcited. The 2π minimum is also sensitive to the pulse shape for off-resonance excitation. Only a hyperbolic secant time dependence is able to return all of the atoms to the ground state for a 2π off-resonance pulse. Consequently, incoherent resonance fluorescence could be useful in determining the area of picosecond pulses, centering them on narrow absorbers, and measuring the dipole moments and relaxation times of the absorber.

---

[1]I. D. Abella, N. A. Kurnit, and S. R. Hartmann, Phys. Rev. 141, 391 (1966).

[2]E. L. Hahn, Phys. Rev. 80, 580 (1950).

[3]S. L. McCall and E. L. Hahn, Phys. Rev. 183, 457 (1969).

[4]R. E. Slusher and H. M. Gibbs, Phys. Rev. A 5, 1634 (1972).

[5]H. P. Grieneisen, N. A. Kurnit, and A. Szöke, Opt. Commun. 3, 259 (1971). They performed a similar experiment in which the fluorescence oscillated very little with input area because of level degeneracies and broadline absorption.

[6]The highlights of this experiment were summarized by H. M. Gibbs [Phys. Rev. Lett. 29, 459 (1972); and in *Coherence and Quantum Optics*, edited by L. Mandel and E. Wolf (Plenum, New York, 1973), p. 83] in which the experimental data are shown to be inconsistent with the Jaynes-Crisp-Stroud neoclassical theory of radiation. Also see the following paper, Phys. Rev. A 8, 456 (1973).

[7]H. M. Gibbs and R. J. Hull, Phys. Rev. 153, 132 (1967).

[8]G. D. Chapman, L. Krause, and I. H. Brockman, Phys. 42, 535 (1964); J. C. Hsieh and J. C. Baird, Phys. Rev. A 3, 141 (1972).

[9]R. H. Dicke, Phys. Rev. 93, 99 (1954); D. C. Burnham and R. Y. Chiao, Phys. Rev. 188, 667 (1969); F. T. Arecchi and E. Courtens, Phys. Rev. A 2, 1730 (1970); Ref. 1.

[10]E. L. Hahn, N. S. Shiren, and S. L. McCall, Phys. Lett. 37A, 265 (1971).